


[View Journal Online](#)
[View Article Online](#)

Green synthesis of silver nano-catalyst using ionic liquid and their photocatalytic application to the reduction of *p*-nitrophenol

 Ravi Ranjan , Durga Gupta  and Madhulata Shukla *

Department of Chemistry, Gram Bharti College, Ramgarh, Kaimur, Veer Kunwar Singh University, 821110, Bihar, India

 * Corresponding author at: Department of Chemistry, Gram Bharti College, Ramgarh, Kaimur, Veer Kunwar Singh University, 821110, Bihar, India.
 e-mail: madhulata.pf.chy17@itbhu.ac.in (M. Shukla).

RESEARCH ARTICLE

ABSTRACT



doi 10.5155/eurjchem.14.3.316-322.2436

 Received: 02 April 2023
 Received in revised form: 28 May 2023
 Accepted: 04 June 2023
 Published online: 30 September 2023
 Printed: 30 September 2023

KEYWORDS

 Ionic liquid
 Nanoparticle
 NBO analysis
 DFT calculation
 Green synthesis
 Photocatalytic reduction

Ionic liquids (ILs) carrying special properties can act as electronic as well as steric stabilisers by preventing nanoparticle (NP) growth and NP aggregation. The effect of visible light on the catalytic properties of silver nanoparticles is a hot topic of extensive research nowadays. The present report demonstrates the current developments in the green synthesis of silver nanoparticles in ionic liquids and a detailed study of the room-temperature catalytic and photocatalytic reduction of *p*-nitrophenol (PNP) to *p*-aminophenol (AP). The Ag nanoparticles (AgNPs) functionalised by ionic liquids are prepared in the 40-140 nm range and are found to be spherical in shape. The photocatalytic properties of these nanocomposites for the reduction of PNP to AP were studied. Photocatalytic degradation of PNP was also analysed by these composite nanostructures. The plasmonic photocatalytic properties of the synthesised AgNPs revealed activity significantly higher than that of the room-temperature catalysis. Density functional theory calculations showed that strong interactions exist between nanoclusters and ILs. Natural bond orbital analysis showed that IL also activates the nanoparticles for further photocatalytic reduction by transferring electron transfer from the donor (IL) to the acceptor (Ag cluster) and activating the silver NPs for further catalytic reaction. Photocatalytic degradation of PNP (reduction of PNP to AP) using NP in the absence of light follows first-order kinetics, whereas in the presence of light it follows zero-order reaction kinetics.

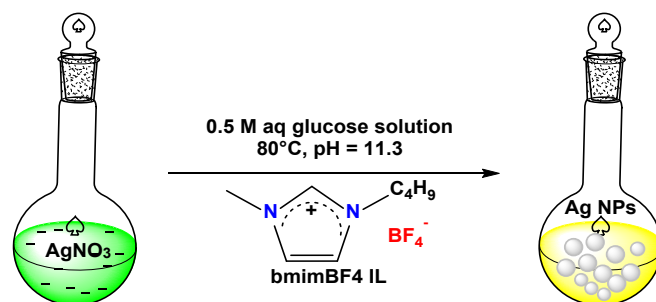
 Cite this: *Eur. J. Chem.* 2023, 14(3), 316-322

 Journal website: www.eurjchem.com

1. Introduction

Research on nanoparticles (NPs) has been of great interest over the past two decades in the field of biomedical, chemical, and material sciences and engineering. The growing application of NPs is mainly due to their interesting and unique properties at the nanolevel compared to those of the bulk composition. Different NPs synthesised using different methodologies have variable shapes, sizes, and morphology and hence lead to a dramatic change in the properties of the synthesised NPs. NPs used in different fields are synthesised specifically, depending on the type of requirement. Hence, nanomaterials are in high demand for practical applications in the fields of medicine, agriculture, *etc.* due to their tunable properties. To date, several reports are available explaining the synthesis of metal nanoparticles in glycerol and other conventional organic solvents [1-4]. Although conventional organic solvents are very toxic to humans and the environment, researchers are moving forward and using green solvents for nanoparticle synthesis nowadays [5]. Ionic liquids have been classified as new materials and have attracted great interest in recent years because of their applications in multidisciplinary areas involved with chemistry, materials science, chemical engineering, environmental science, physics, and biology. A smart combination of ILs and unconventional synthesis methods allows added value to

be drawn from the extensive environment of available property combinations. ILs are used as green solvents for the synthesis of nanomaterials due to their favourable chemical and physical properties [6,7]. Synthesis conditions with high reaction and nucleation rates can be attained, which leads to the formation of extremely small nanoparticles. ILs act as electronic as well as steric stabilisers preventing nanoparticle (NP) growth and nanoparticle aggregation. The effect of impurities, as well as water present in ILs, also plays an important role in determining the structure, shape, size, and morphology of synthesised NPs. ILs at room temperature were used to synthesise size-controlled nanoparticles [8,9]. ILs form protective layers on metal surfaces. As reported earlier, metal NPs are electron-deficient [10,11], therefore negatively charged anions tend to interact with their surface to form electrical double layers with oppositely charged cations [12]. Repulsion encounter between the outer cationic layers avoids NP agglomeration. Another way to control the agglomeration is to provide steric hindrance by the alkyl chains present in the cations, which proficiently limit the physical contact between the NPs. It is a well-known fact and reported in the literature that electrostatic interaction is dominant if ILs contain a short to medium length alkyl chain in the cationic part. And as the chain length increases, the van der Waals interaction competes predominantly with electrostatic interactions [13].



Scheme 1. Synthesis of silver nanoparticles in 1-butyl-3-methylimidazolium tetrafluoroborate IL.

Because of the larger size of the alkyl chain present in ILs, it prevents one smaller nanoparticle formed in the solution from coming closer to another one and hence prevents the aggregation of smaller-sized nanoparticles. The consequent dynamic network comprising Coulomb forces and hydrogen bonds between the ions avoids the agglomeration of NPs without affecting their mobility [14,15]. In the case of imidazolium ILs, the surface organisation depends mainly on its composition and ion orientation [3,15]. The significant chemical tunability of the ILs allows variation of the stability, geometry, and electronic properties of the catalyst. With slight variation in the alkyl group or anion, the properties of ILs can be tuned very differently and the different ILs used for the synthesis of NP will definitely affect the properties of synthesised NP as well, because it was reported by us in our previous finding that IL decreases the band gap between NPs and initiates the catalytic properties [16]. The preparation of metal NPs in ILs appears extremely practical. NPs can be synthesised by physical and chemical means, including chemical reduction, sputtering, and decomposition, etc. [3,17-20]. Silver nanoparticles are recognised for their numerous physical, biological, and pharma-ceutical applications, comprising medicinal ones such as biomolecular detection and drug delivery carriers. They also serve as antibacterial, antiviral, and antifungal agents [21]. Liu *et al.* in 2020 reported the synthesis of silver NPs in glycerol at room temperature, neutral pH conditions, and in the absence of ultraviolet radiation. They have reported that aldehydes and free radicals generated from glycerol act as the reducing agent used for the synthesis of silver NP [22]. Imidazolium ILs have been reported to be superior, medium, and better reaction conditions for the synthesis of silver, gold, and copper NPs [23]. In the earlier literature, silver ions have been reported to interact with sodium hydroxide (NaOH) and form silver oxide (Ag_2O) NPs which is then reduced to silver NP using NaBH_4 as a reducing agent [24]. Another report by Fang *et al.* explaining the formation of Ag_2O mesocages in alkaline medium that is reduced to silver mesocages using hydrogen peroxide (H_2O_2) as a reducing agent is also available [25]. Similarly, many more research papers are available explaining the reduction of Ag_2O to Ag and the NPs obtained are of spherical and regular shape and size [26,27]. Benet *et al.* have also reported that the reaction for the synthesis of silver NPs is faster under alkali conditions (pH >10) [28]. Taking into account all relevant research articles, the final conclusion was planned to advance for the synthesis of silver NP under alkaline conditions in the presence of glucose and 1-butyl-3-methylimidazolium tetrafluoro borate (bmimBF₄) ionic liquid. In the present study, the synthesis of silver NPs using a novel method has been reported and the synthesised NP shows tremendous photocatalytic activity studied for reducing *p*-nitrophenol (PNP) to aminophenol (AP). Natural-bond orbital (NBO) analysis showed that IL activates the nanoparticles by supplying electrons to the nanocluster for further photocatalytic reduction. The photo-

catalytic properties of the synthesised AgNPs revealed significantly more activity compared to that of the room-temperature catalysis.

2. Experimental

The materials used for the synthesis of silver nanoparticles were silver nitrate, AgNO_3 (Merck, CAS No- 7761-88-8), 1-butyl-3-methylimidazolium tetrafluoroborate, bmimBF₄ (IoliTech, CAS No- 174501-65-6), and glucose (Merck, CAS No- 50-99-7). All reagents were used as received without further purification.

2.1. Synthesis of silver nanoparticles using bmimBF₄ ionic liquid

The schematic diagram for the synthesis of AgNP in bmimBF₄ IL is shown in Scheme 1. 25 ml of 0.1 M AgNO_3 solution (in water) was taken in a round bottom flask. The reaction mixture was kept in a water bath whose temperature was maintained at 80 °C. Dropwise 2 ml of bmimBF₄ IL was added with continuous stirring. The stirring was continued for 30 minutes. 15 mL of 0.5 M glucose (in aqueous solution) was added with stirring at the same temperature. Stirring was carried out for 20 min at this temperature. The colour of the solution changes from colourless to light grey. After that 5 ml 1 M NaOH was added to gain the pH of approximately 11.3, stirring was performed at the same constant temperature of 80 °C for one and a half hours. The colour of the solution changes to grey. The solution was centrifuged, and the sample was washed well with ethanol. Dried in a vacuum oven for 2 days. UV visible spectra were recorded and a sharp peak was observed at a maximum of 423 nm.

2.2. Characterisation

Different characterisation techniques were performed to analyse the size, morphology, and composition of the nanoparticles produced. X-ray diffraction measurements were performed by Rigaku Mini-X 600, Japan. Transmission electron microscopy imaging and electron diffraction of as-prepared silver NPs were performed with a TECNAI 20 G2-electron microscope operating at a voltage of 200 kV. The Agilent Cary 60 spectrophotometer was used to record the UV-visible absorption spectra of the sample dispersed in an aqueous medium.

2.3. Computational details

The materials and processes simulator (Scienomics, MAPS software) [29] was used to carve out the FCC Ag lattice nanocluster. DFT calculations at Beck's three functional parameters and Lee-Yang-Parr hybrid functional (B3LYP) level [30,31] of calculation were carried out using the Gaussian 16 program [32].

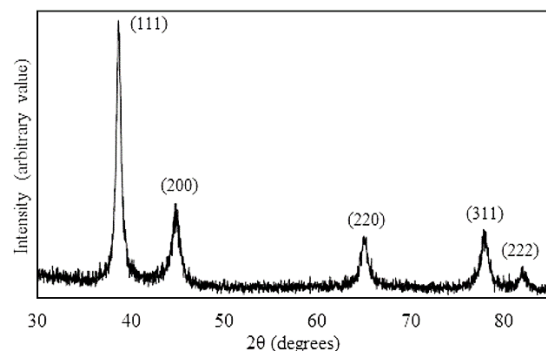


Figure 1. XRD pattern of silver NPs.

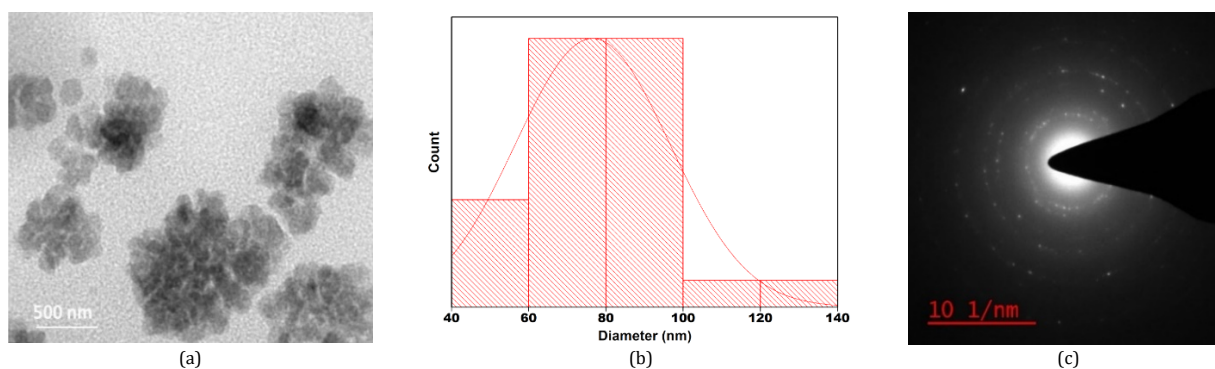


Figure 2. (a) TEM image of AgNP stabilized by bmimBF₄ IL, (b) size distribution curve and (c) selected area electron diffraction pattern.

LANL2DZ basis set [33] was used for silver atom and 6-31G++(d,p) basis set for C, H, N, O, B, and F atoms. The literature survey illustrates that the B3LYP level of calculations gives a stable cluster at the ground state [2,16,34]. Calculations were carried out for the optimisation of the ground state geometry in the gaseous phase. The natural bond orbital (NBO) analysis was performed at the same level of calculation and using a similar basis set as that for geometry optimization. NBO has been carried out to find the second-order perturbation stabilisation energy and to find the donor-acceptor interactions in the bmimBF₄-Ag cluster system.

3. Results and discussion

3.1 Characterisation of AgNPs

3.1.1. XRD measurements

Figure 1 shows the X-ray diffraction pattern of the powdered AgNP sample. Five peaks were observed at 38.18, 44.41, 64.67, 77.07, and 81.25° which correspond to {111}, {200}, {220}, {311}, and {222} reflections, respectively, of FCC silver in JCPDS-ICDD (Card no. 87-0720). The same peaks for silver nanoparticles have been reported in many of the literatures earlier [35,36]. Thus, the FCC Ag phase was formed under the synthesis conditions used.

3.1.2. TEM measurements

The TEM micrograph of the AgNP sample and its corresponding electron diffraction pattern are shown in Figure 2. Figure 2a shows a bright-field TEM image of AgNPs stabilised with bmimBF₄ IL. Mostly, the observed particles are spherical in shape with sizes ranging from 40-140 nm. The size distribution curve is shown in Figure 2b. The electron diffraction ring pattern, shown in Figure 2c, indicates the FCC Ag lattice. This confirms the formation of IL-stabilised AgNPs.

3.1.3. UV-vis spectra

The UV-visible spectrum of the IL-AgNPs dispersion prepared by the protocol given in Scheme 1 is shown in Figure 3. The maximum absorbance peak in the spectrum of the prepared dispersion is located at about 423 nm. This is characteristic of the localised surface plasmon resonance absorption due to AgNPs as reported in many of the literatures [2,37].

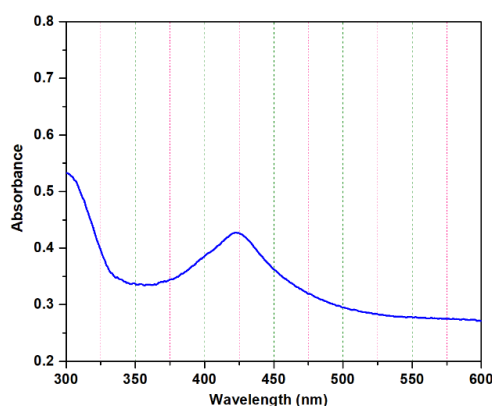
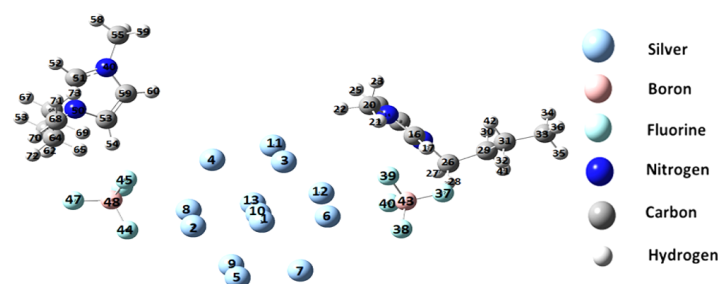
3.2. NBO analysis

Geometry optimisation, frequency calculation, and time-dependent DFT (TD-DFT) calculations of the Ag₁₃-bmimBF₄ cluster have been carried out by us previously and have been reported elsewhere [16]. The optimised structure of the Ag₁₃-bmimBF₄ cluster calculated at the B3LYP level of calculation and using the LANL2DZ basis set was used for the silver atom and the 6-31G++(d,p) basis set for the C, H, N, O, B, and F atoms shown in Figure 4. The natural bond orbital (NBO) calculation is an effective tool to understand the intermolecular hydrogen bond [38-40]. To gain a deeper understanding of the interactions in the bmimBF₄-Ag cluster, an NBO analysis was performed on the optimised geometry. The electron acceptor orbitals, electronic donor orbitals, and their corresponding second-order perturbation stabilisation energy E(2), related to the delocalisation tendency of electrons from donor to acceptor orbitals, are tabulated and shown in Table 1.

The intermolecular electron transfer occurs from lone pair LP(F) orbitals to the antibonding σ*(C53-H54 and C16-H17) orbitals with the corresponding E(2) values 3.27 and 3.02, respectively, which can well confirm the hydrogen bonds of C-H...F between the cation and anion in ILs. It is well known that intermolecular orbital interactions can be estimated by the magnitude of E(2), the higher value of E(2) indicates a stronger interaction between the donor and the acceptor [38-40].

Table 1. Donor-acceptor interactions in the bmimBF₄-Ag cluster system and second-order perturbation stabilisation energies (E(2), kcal/mol).

Donor (E _i)	Acceptor (E _j)	Second-order perturbation stabilisation energy E(2) (kcal/mol)
LP (3) F46	BD*(1) C53 - H54	3.27
LP (3) F37	BD*(1) C16 - H17	3.02
LP (1) F46	LP*(8)Ag8	4.18
LP (1) F44	LP*(9)Ag8	1.92
BD (1) F46 - B48	LP*(8)Ag8	3.30
LP (1) F45	LP*(7)Ag4	2.29
LP (1) F45	LP*(7)Ag2	2.77
LP (1) F44	LP*(8)Ag2	2.52
BD (1) F44 - B48	LP*(8)Ag2	2.05
LP (3) F40	LP*(6)Ag12	2.59
LP (1) F40	LP*(8)Ag12	5.46
BD (1) F40 - B43	LP*(8)Ag12	1.72
BD (1) F39 - B43	LP*(8)Ag12	1.77
LP (1) F39	LP*(8)Ag6	2.77
LP (1) F38	LP*(8)Ag6	3.41
BD (1) F40 - B43	LP*(8)Ag6	2.57
BD (1) F39 - B43	LP*(8)Ag6	1.92
BD (1) F38 - B43	LP*(8)Ag6	1.89

**Figure 3.** UV-vis spectrum of AgNP synthesised using bmimBF₄ IL.**Figure 4.** Optimised geometry of the Ag₁₃-bmimBF₄ cluster. Different colours representing different atoms are shown above.

From Table 1, one can find that the LP(F) → LP*(Ag) interactions show higher E(2) values compared to the C-H interaction with Ag (all values observed to be less than 1 kcal/mol, hence not reported in Table 1) suggesting that the LP(F) → LP*(Ag) interactions are stronger in the bmimBF₄-Ag system. This also indicates that the Ag cluster is surrounded mostly by anions rather than cations. This statement has also been verified from the available previous literature [16]. As a consequence of electron transfer from bmimBF₄ IL to Ag cluster, NP gets activated and proceeds for photocatalytic reaction.

3.3. Catalytic PNP reduction

2 mL of water and 200 μL of PNP solution were mixed in a standard quartz cuvette of 1 cm path length. The UV-vis spectrum of this reaction mixture (without catalyst) was recorded. The concrete experiment was then carried out in the presence of catalyst (5 mg in 2 ml of water) with the reaction

mixture (2 ml of water + 200 μL PNP + 5 μL HCl + 50 μL Ag NP + 50 μL H₂O₂) at room temperature. Its UV-visible spectrum was recorded every five minutes and is shown in Figure 5.

The plot of absorbance (A) vs. time (t) and ln [A] vs. time for reaction under normal conditions is shown in Figures 6a and 6b, respectively. From Figures 6a and 6b, it is clear that the kinetics follows first-order reactions under normal conditions. Similar experimental results on silver nanoparticles have been analysed in many of the literature [41].

The UV-vis spectrum of PNP hydrogenation in the presence of silver catalyst and light is shown in Figure 7. The photocatalytic reaction was carried out under visible light irradiation with the reaction mixture of 2 ml of water + 200 μL PNP + 5 μL HCl + 50 μL Ag NP + 50 μL H₂O₂ at room temperature. Its UV-visible spectrum was recorded every five minutes and is shown in Figure 7. Similar photochemical degradation of nitrophenol using silver nanoparticles has been analysed in many of the literature [2,41,42].

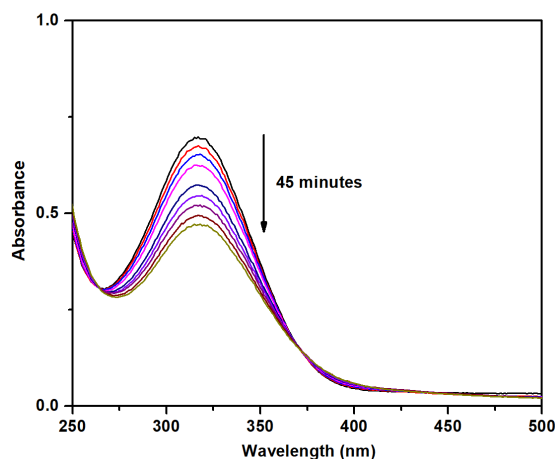


Figure 5. UV-vis spectra of hydrogenation of PNP in the presence of Ag NP.

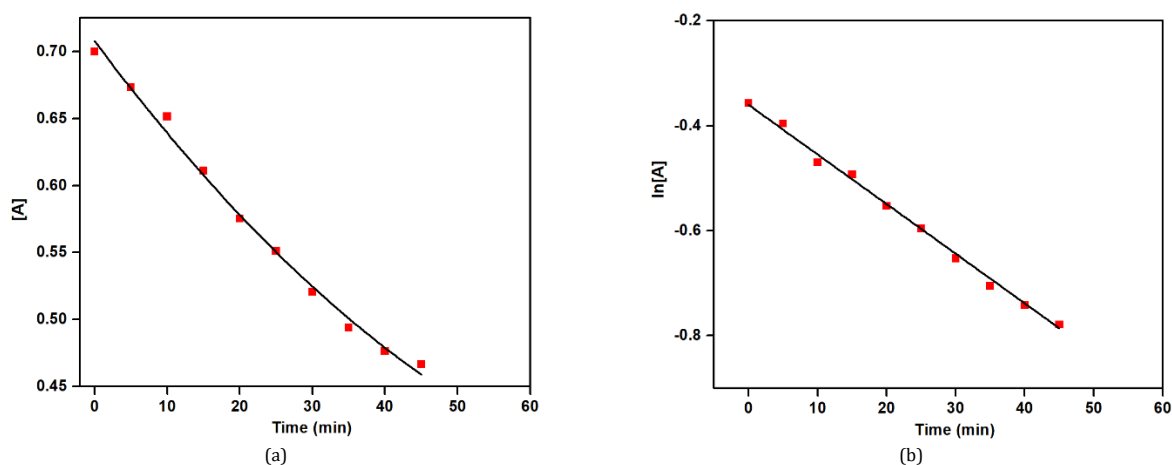


Figure 6. (a) Variation of A [absorbance (A) measured at ~ 317 nm] vs time and (b) $\ln[A]$ vs time in photocatalytic PNP reduction using NP. The R^2 value of both fittings is ~ 0.998 .

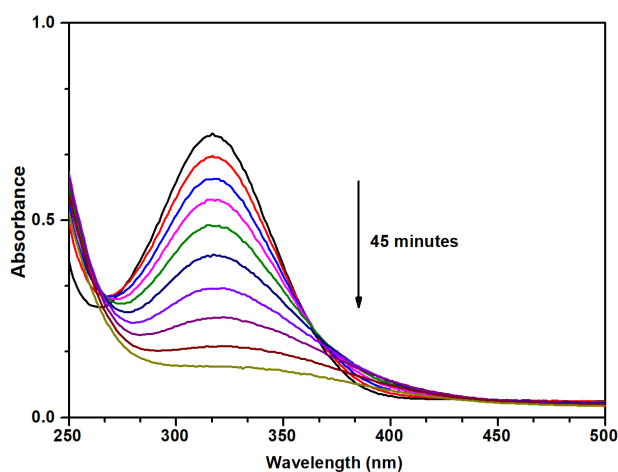


Figure 7. UV-vis spectra of hydrogenation of PNP in the presence of AgNP (Photocatalytic reaction).

The plot of absorbance (A) vs. time (t) and $\ln[A]$ vs. time for photocatalytic reaction is shown in Figures 8a and 8b, respectively. From Figures 8a and 8b, it is clear that the kinetics follow a zero-order reaction when irradiated with visible light.

The discussion above gives a qualitative analysis of the changes in catalytic activity when the reaction is carried out at normal room temperature and in visible light irradiation. A

more quantitative understanding can be obtained from the degradation kinetics. Figures 6 and 8 show the kinetics of PNP degradation under normal and visible light irradiation conditions. The PNP degradation followed first-order kinetics in the absence of visible-light irradiation. However, PNP degradation follows zero-order kinetics under visible light irradiation.

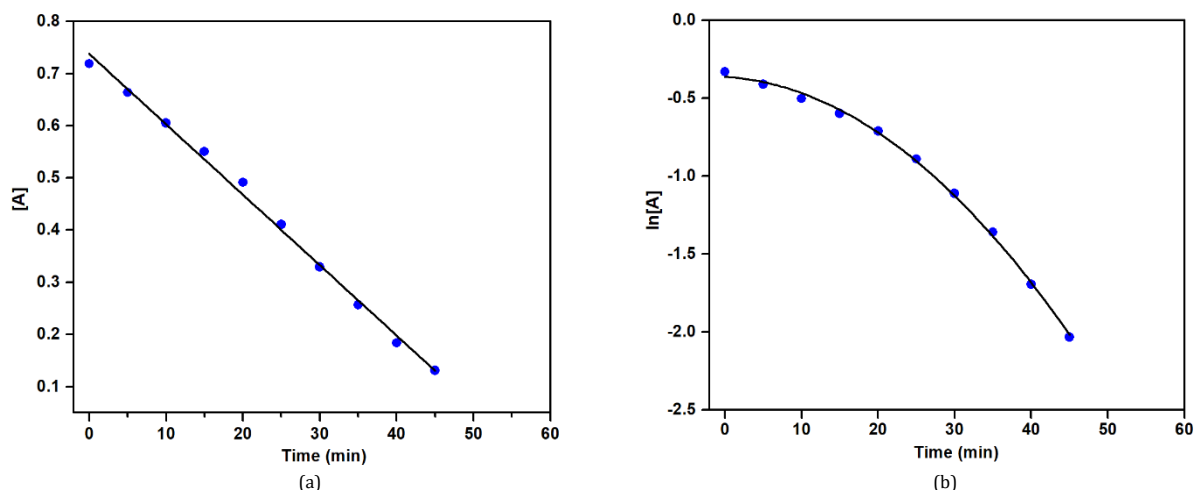


Figure 8. (a) Variation of A [absorbance (A) measured at ~ 317 nm] vs time and (b) $\ln[A]$ vs time in photocatalytic PNP reduction using NP in presence of light. The R^2 value of both fittings is ~ 0.99 . Kinetics follows a zero-order reaction.

We cannot compare the rate constants of the catalytic kinetics that follow different orders, as they have different units and they are not comparable. The photocatalytic PNP degradation followed zero-order kinetics (shown in Figures 8a and 8b), contrary to the kinetics exhibited in the absence of visible light irradiation (shown in Figures 6a and 6b). The change in reaction kinetics order indicated a difference in the catalytic mechanism due to light irradiation.

4. Conclusions

Silver nanoparticles were prepared using a green reduction methodology using 1-butyl-3-methylimidazolium tetrafluoroborate and a detailed study has been done on the effect of IL on the size and photocatalytic activity of AgNP. The photocatalytic activity toward PNP reduction was evaluated in the absence and in the presence of visible light irradiation. PNP degradation was observed to be very slow in the absence of light, whereas visible light irradiation significantly boosted the reaction kinetics. NBO analysis was performed and found to show a strong interaction between the Ag cluster and bmimBF₄ IL through BF₄⁻ anion. Also, electron transfer from the donor (ILs) to the acceptor (Ag cluster) indicates that ILs stimulate the NP for the further catalytic reaction. Photocatalytic PNP reduction using NP in the absence of light follows first-order kinetics, whereas in the presence of light it follows zero-order reaction kinetics.

Disclosure statement

Conflict of interest: The authors declare that they have no conflict of interest. Ethical approval: All ethical guidelines have been adhered. Sample availability: Samples of the compounds are available from the author.

CRedit authorship contribution statement

Conceptualization: Ravi Ranjan, Durga Gupta and Madhulata Shukla; Methodology: Durga Gupta; Software: Ravi Ranjan; Formal analysis: Ravi Ranjan and Durga Gupta; Validation: Ravi Ranjan and Durga Gupta; Investigation: Ravi Ranjan and Durga Gupta; Data Curation: Durga Gupta; Writing - Original Draft: Durga Gupta; Writing - Review and Editing: Ravi Ranjan, Supervision: Madhulata Shukla; Project Administration: Madhulata Shukla. Both authors Ravi Ranjan and Durga Gupta contributed equally to write the manuscript.

Acknowledgements


Madhulata Shukla acknowledges financial assistance from UGC, India (F.30-446/2018 (BSR)). The authors thank the Central Instrument Facility, Indian

Institute of Technology, Banaras Hindu University, India, for characterisation facilities and Centre for Computing and Information Services, Indian Institute of Technology, Banaras Hindu University, India, for computational facilities.

ORCID and Email

Ravi Ranjan

 raviranjangbcr@gmail.com

 <https://orcid.org/0009-0004-3720-4514>

Durga Gupta


 gdurga813@gmail.com

 <https://orcid.org/0009-0003-6296-5131>

Madhulata Shukla

 madhu1.shukla@gmail.com

 madhulata.pf.chy17@itbhu.ac.in

 <https://orcid.org/0000-0002-4060-8729>

References

- [1]. Kumar, S.; Kuntail, J.; Sahu, D. K.; Yadav, V. S.; Sinha, I. Green synthesis of curcumin functionalized Au nanoparticles by visible light photo-reduction. *Indian J. Phys. Proc. Indian Assoc. Cultiv. Sci.* (2004) **2023**, <https://doi.org/10.1007/s12648-023-02617-y>.
- [2]. Verma, A.; Shukla, M.; Kumar, S.; Pal, S.; Sinha, I. Mechanism of visible light enhanced catalysis over curcumin functionalized Ag nanocatalysts. *Spectrochim. Acta A Mol. Biomol. Spectrosc.* **2020**, *240*, 118534.
- [3]. Janiak, C. Ionic liquids for the synthesis and stabilization of metal nanoparticles. *Z. Naturforsch. B J. Chem. Sci.* **2013**, *68*, 1059–1089.
- [4]. Gautam, P.; De, A. K.; Sinha, I.; Behera, C. K.; Singh, K. K. Genesis of copper oxide nanoparticles from waste printed circuit boards and evaluation of their photocatalytic activity. *Environ. Res.* **2023**, *229*, 115951.
- [5]. Endres, F. Physical chemistry of ionic liquids. *Phys. Chem. Chem. Phys.* **2010**, *12*, 1648.
- [6]. Marcos Esteban, R.; Meyer, H.; Kim, J.; Gemel, C.; Fischer, R. A.; Janiak, C. Comparative synthesis of Cu and Cu₂O nanoparticles from different copper precursors in an ionic liquid or propylene carbonate. *Eur. J. Inorg. Chem.* **2016**, *2016*, 2106–2113.
- [7]. Shukla, M.; Srivastava, N.; Sah, S. Interactions and transitions in imidazolium cation based ionic liquids. In *Ionic Liquids - Classes and Properties*; InTech, 2011.
- [8]. Swadźba-Kwaśny, M.; Chancelier, L.; Ng, S.; Manyar, H. G.; Hardacre, C.; Nockemann, P. Facile in situ synthesis of nanofluids based on ionic liquids and copper oxide clusters and nanoparticles. *Dalton Trans.* **2012**, *41*, 219–227.
- [9]. Ma, Q.; Ping, L.; Zhang, H. M.; Yang, J.; Wang, Q. Ionic liquid synthesis of luminescent nano-cubes and their microstructure characterization. *J. Mol. Struct.* **2015**, *1091*, 1–5.
- [10]. Watzky, M. A.; Finke, R. G. Transition metal nanocluster formation kinetic and mechanistic studies. A new mechanism when hydrogen is the reductant: Slow, continuous nucleation and fast autocatalytic surface growth. *J. Am. Chem. Soc.* **1997**, *119*, 10382–10400.

- [11]. Scheeren, C. W.; Machado, G.; Teixeira, S. R.; Morais, J.; Domingos, J. B.; Dupont, J. Synthesis and characterization of pt(0) nanoparticles in imidazolium ionic liquids. *J. Phys. Chem. B* **2006**, *110*, 13011–13020.
- [12]. He, Z.; Alexandridis, P. Nanoparticles in ionic liquids: interactions and organization. *Phys. Chem. Chem. Phys.* **2015**, *17*, 18238–18261.
- [13]. Bhargava, B. L.; Balasubramanian, S.; Klein, M. L. Modelling room temperature ionic liquids. *Chem. Commun. (Camb.)* **2008**, 3339–3351.
- [14]. Capece, A. Synthesis of silver nanoparticles in ionic liquids by electron irradiation. *APS* **2018**, LW1.072.
- [15]. Shipway, A. N.; Katz, E.; Willner, I. Nanoparticle arrays on surfaces for electronic, optical, and sensor applications. *Chemphyschem* **2000**, *1*, 18–52.
- [16]. Shukla, M.; Verma, A.; Kumar, S.; Pal, S.; Sinha, I. Experimental and DFT calculation study of interaction between silver nanoparticle and 1-butyl-3-methyl imidazolium tetrafluoroborate ionic liquid. *Heliyon* **2021**, *7*, e06065.
- [17]. Migowski, P.; Machado, G.; Teixeira, S. R.; Alves, M. C. M.; Morais, J.; Traverse, A.; Dupont, J. Synthesis and characterization of nickel nanoparticles dispersed in imidazolium ionic liquids. *Phys. Chem. Chem. Phys.* **2007**, *9*, 4814–4821.
- [18]. Ruta, M.; Laurenczy, G.; Dyson, P. J.; Kiwi-Minsker, L. Pd nanoparticles in a supported ionic liquid phase: Highly stable catalysts for selective acetylene hydrogenation under continuous-flow conditions. *J. Phys. Chem. C Nanomater. Interfaces* **2008**, *112*, 17814–17819.
- [19]. Redel, E.; Thomann, R.; Janiak, C. First correlation of nanoparticle size-dependent formation with the ionic liquid anion molecular volume. *Inorg. Chem.* **2008**, *47*, 14–16.
- [20]. Wender, H.; Migowski, P.; Feil, A. F.; Teixeira, S. R.; Dupont, J. Sputtering deposition of nanoparticles onto liquid substrates: Recent advances and future trends. *Coord. Chem. Rev.* **2013**, *257*, 2468–2483.
- [21]. Gholami, A.; Shams, M. S.; Abbaszadegan, A.; Nabavizadeh, M. Ionic liquids as capping agents of silver nanoparticles. Part II: Antimicrobial and cytotoxic study. *Green Process. Synth.* **2021**, *10*, 585–593.
- [22]. Liu, T.; Baek, D. R.; Kim, J. S.; Joo, S.-W.; Lim, J. K. Green synthesis of silver nanoparticles with size distribution depending on reducing species in glycerol at ambient pH and temperatures. *ACS Omega* **2020**, *5*, 16246–16254.
- [23]. Wang, W.; Peng, X.; Xiong, H.; Wen, W.; Bao, T.; Zhang, X.; Wang, S. Synthesis and properties enhancement of metal nanoclusters templated on a biological molecule/ionic liquids complex. *New J Chem* **2017**, *41*, 3766–3772.
- [24]. Jo, J.; Cho, S.-P.; Lim, J. K. Template synthesis of hollow silver hexapods using hexapod-shaped silver oxide mesoparticles. *J. Colloid Interface Sci.* **2015**, *448*, 208–214.
- [25]. Fang, J.; Liu, S.; Li, Z. Polyhedral silver mesocages for single particle surface-enhanced Raman scattering-based biosensor. *Biomaterials* **2011**, *32*, 4877–4884.
- [26]. Zhang, X.; Hicks, E. M.; Zhao, J.; Schatz, G. C.; Van Duyne, R. P. Electrochemical tuning of silver nanoparticles fabricated by nanosphere lithography. *Nano Lett.* **2005**, *5*, 1503–1507.
- [27]. Gomes, J. F.; Garcia, A. C.; Ferreira, E. B.; Pires, C.; Oliveira, V. L.; Tremiliosi-Filho, G.; Gasparotto, L. H. S. New insights into the formation mechanism of Ag, Au and AgAu nanoparticles in aqueous alkaline media: alkoxides from alcohols, aldehydes and ketones as universal reducing agents. *Phys. Chem. Chem. Phys.* **2015**, *17*, 21683–21693.
- [28]. Benet, W. E.; Lewis, G. S.; Yang, L. Z.; Hughes, D. E. P. The mechanism of the reaction of the Tollens reagent. *J. Chem. Res.* **2011**, *35*, 675–677.
- [29]. Materials and Processes Simulations Platform, Version 4.2, Scienomics SARL, Paris, France.
- [30]. Lee, C.; Yang, W.; Parr, R. G. Development of the Colle-Salvetti correlation-energy formula into a functional of the electron density. *Phys. Rev. B Condens. Matter* **1988**, *37*, 785–789.
- [31]. Becke, A. D. Density-functional thermochemistry. III. The role of exact exchange. *J. Chem. Phys.* **1993**, *98*, 5648–5652.
- [32]. Frisch, M. J.; Trucks, G. W.; Schlegel, H. B.; Scuseria, G. E.; Robb, M. A.; Cheeseman, J. R.; Montgomery, J. A.; Vreven, T.; Kudin, K. N.; Burant, J. C.; Millam, J. M.; Iyengar, S. S.; Tomasi, J.; Barone, V.; Mennucci, B.; Cossi, M.; Scalmani, G.; Rega, N.; Petersson, G. A.; Nakatsuji, H.; Hada, M.; Ehara, M.; Toyota, K.; Fukuda, R.; Hasegawa, J.; Ishida, M.; Nakajima, T.; Honda, Y.; Kitao, O.; Nakai, H.; Klene, M.; Li, X.; Knox, J. E.; Hratchian, H. P.; Cross, J. B.; Adamo, C.; Jaramillo, J.; Gomperts, R.; Stratmann, R. E.; Yazyev, O.; Austin, A. J.; Cammi, R.; Pomelli, C.; Ochterski, J. W.; Ayala, P. Y.; Morokuma, K.; Voth, G. A.; Salvador, P.; Dannenberg, J. J.; Zakrzewski, V. G.; Dapprich, S.; Daniels, A. D.; Strain, M. C.; Farkas, O.; Malick, D. K.; Rabuck, A. D.; Raghavachari, K.; Foresman, J. B.; Ortiz, J. V.; Cui, Q.; Baboul, A. G.; Clifford, S.; Cioslowski, J.; Stefanov, B. B.; Liu, G.; Liashenko, A.; Piskorz, P.; Komaromi, I.; Martin, R. L.; Fox, D. J.; Keith, T.; Al-Laham, M. A.; Peng, C. Y.; Nanayakkara, A.; Challacombe, M.; Gill, P. M. W.; Johnson, B.; Chen, W.; Wong, M. W.; Gonzalez, C.; Pople, J. A. Gaussian, Inc., Gaussian 16, Revision C.01, Wallingford CT, 2016.
- [33]. Hay, P. J.; Wadt, W. R. Ab initio effective core potentials for molecular calculations. Potentials for the transition metal atoms Sc to Hg. *J. Chem. Phys.* **1985**, *82*, 270–283.
- [34]. Verma, A.; Gupta, R. K.; Shukla, M.; Malviya, M.; Sinha, I. Ag-Cu bimetallic nanoparticles as efficient oxygen reduction reaction electrocatalysts in alkaline media. *J. Nanosci. Nanotechnol.* **2020**, *20*, 1765–1772.
- [35]. Singh, R.; Sahu, S. K.; Thangaraj, M. Biosynthesis of silver nanoparticles by marine invertebrate (polychaete) and assessment of its efficacy against human pathogens. *J. Nanoparticles* **2014**, *2014*, 1–7.
- [36]. Theivasanthi, T.; Alagar, M. Electrolytic synthesis and characterizations of silver nanopowder. **2011**, <https://arxiv.org/abs/1111.0260>.
- [37]. Verma, A. D.; Jain, N.; Singha, S. K.; Quraishi, M. A.; Sinha, I. Green synthesis and catalytic application of curcumin stabilized silver nanoparticles. *J. Chem. Sci. (Bangalore)* **2016**, *128*, 1871–1878.
- [38]. Reed, A. E.; Curtiss, L. A.; Weinhold, F. Intermolecular interactions from a natural bond orbital, donor-acceptor viewpoint. *Chem. Rev.* **1988**, *88*, 899–926.
- [39]. Weinhold, F.; Landis, C. R.; Glendening, E. D. What is NBO analysis and how is it useful? *Int. Rev. Phys. Chem.* **2016**, *35*, 399–440.
- [40]. Shukla, M.; Sinha, I. Catalytic activation of nitrobenzene on PVP passivated silver cluster: A DFT investigation. *Int. J. Quantum Chem.* **2018**, *118*, e25490.
- [41]. Kästner, C.; Thünemann, A. F. Catalytic reduction of 4-nitrophenol using silver nanoparticles with adjustable activity. *Langmuir* **2016**, *32*, 7383–7391.
- [42]. Shimoga, G.; Palem, R. R.; Lee, S.-H.; Kim, S.-Y. Catalytic degradability of p-nitrophenol using ecofriendly silver nanoparticles. *Metals (Basel)* **2020**, *10*, 1661.



Copyright © 2023 by Authors. This work is published and licensed by Atlanta Publishing House LLC, Atlanta, GA, USA. The full terms of this license are available at <http://www.eurjchem.com/index.php/eurjchem/pages/view/terms> and incorporate the Creative Commons Attribution-Non Commercial (CC BY NC) (International, v4.0) License (<http://creativecommons.org/licenses/by-nc/4.0>). By accessing the work, you hereby accept the Terms. This is an open access article distributed under the terms and conditions of the CC BY NC License, which permits unrestricted non-commercial use, distribution, and reproduction in any medium, provided the original work is properly cited without any further permission from Atlanta Publishing House LLC (European Journal of Chemistry). No use, distribution, or reproduction is permitted which does not comply with these terms. Permissions for commercial use of this work beyond the scope of the License (<http://www.eurjchem.com/index.php/eurjchem/pages/view/terms>) are administered by Atlanta Publishing House LLC (European Journal of Chemistry).